Scanning tunneling microscopy studies of C_{60} monolayers on Au(111)

J. A. Gardener,* G. A. D. Briggs, and M. R. Castell†
Department of Materials, University of Oxford, Parks Road, Oxford OX1 3PH, United Kingdom
(Received 23 July 2009; revised manuscript received 1 December 2009; published 30 December 2009)

We report a scanning tunneling microscopy study of close packed C_{60} monolayers on Au(111) upon post-deposition annealing. Within these structures the C_{60} molecules appear discretely bright or dim. The arrangements of dim C_{60} within the close packed structures are dependent on the orientation of the overlayer with respect to the Au(111) surface. The apparent height difference between the bright and dim C_{60} varies with applied sample bias, and the individual C_{60} molecules can switch from bright-to-dim or vice versa at room temperature. We propose that the dim C_{60} arise from a restructuring of the C_{60}-Au interface to form nanopits, which facilitate charge transfer from the substrate to the first layer fullerene molecules.

DOI: 10.1103/PhysRevB.80.235434 PACS number(s): 68.35.bp, 68.37.Ef, 73.61.Wp, 68.35.Ct

I. INTRODUCTION

Fullerenes are an archetypal molecular system, in which carbon atoms form three-dimensional closed-cage structures. Among this class of materials, C_{60} was the first to be discovered[1] and is the most widely studied. Many investigations into the self-assembly of submonolayer coverage of C_{60} on a wide range of metallic and semiconducting substrates have been performed, and the field has been extensively reviewed.[2] When deposited onto metallic surfaces at room temperature, these molecules generally form close packed islands, often nucleated at substrate step edges. The nature of the interaction between C_{60} and the surface varies between different substrates and plays an important role in the properties of the molecular layer formed. In many cases charge is transferred from the substrate to the fullerene cage, a signature of chemisorption. The amount of charge accepted by C_{60} monolayers varies for different metallic substrates.[3–15]

Differences in the apparent height of features measured by scanning tunneling microscopy (STM) reflect local electronic and/or topographic variations. On some metallic surfaces, particularly after post-deposition annealing, relatively high densities of apparently lower C_{60} molecules can be observed by STM. These so-called "bright" and "dim" C_{60} have been attributed to a C_{60}-induced reconstruction of a range of surfaces, including Ag(100),[16–21] Cu(111),[22] Cu(100),[23] Ni(110),[24] Pt(111),[25] Au(110),[26–28] and Pd(110).[29,30] Such reconstructions can lead to two topographically different C_{60} adsorption sites. Other explanations that have been offered for this height contrast include electronic and molecular orientation effects.[17,31–33] The differing views on the mechanisms behind the bright-dim contrast have meant that this topic remains an active area of investigation.

The most energetically favorable atomic arrangement of a clean Au(111) surface is the "herringbone" $22\times\sqrt{3}$ reconstruction. When deposited via sublimation onto this surface, C_{60} molecules generally lift the Au(111) $22\times\sqrt{3}$ reconstruction and readily form large ordered islands. Within these islands, in the absence of an annealing step, the fullerenes largely appear identical, although occasional isolated dim fullerenes are seen by STM. The C_{60} domains can take on different orientations with respect to the substrate, often adopting the so-called "in phase" 38×38 or $2\sqrt{3}\times2\sqrt{3}R30°$ arrangement.[34] Recently, a phase in which the molecular overlayer is rotated by 14° with respect to the $[10\bar{1}]$ directions of the Au(111) surface has been reported.[35,36] In this arrangement, on average every seventh C_{60} appears dim, giving rise to a quasiperiodic 7×7 superstructure within the fullerene layer. Dim C_{60} on Au(111) have been attributed to impurities,[34] C_{60} molecules of different orientation,[32,33] the occupation of different lattice sites,[11] and a C_{60}-induced modification of the surface.[35–37] Further discrepancies in the literature exist over whether charge transfer occurs between the Au substrate and C_{60} molecules. Localized scanning tunneling spectroscopy studies and some theoretical modeling investigations suggest that no net charge is transferred,[3,38] while photoelectron spectroscopy measurements[6,7] and other theoretical simulations[11] indicate that C_{60} monolayers accept charges of 0.8–1.0 electrons per molecule.

Here, we present a systematic study of C_{60} monolayer growth on Au(111). Our aim is to elucidate the origins of the dim C_{60} molecules on this surface and to resolve the conflicting reports of whether or not charge transfer occurs. Inspired by the aforementioned thermally induced bright-dim C_{60} arrays created on other metallic surfaces,[16–30] we have chosen to study annealed submonolayer films on Au(111). We find that different domains can exist comprising a range of densities and arrangements of dim C_{60}. Our analyses allow us to propose a model in which nanopits are formed at the Au(111)-C_{60} interface which promote charge transfer from the substrate to the fullerene layer.

II. EXPERIMENTAL

Thin Au(111) on mica films were Ar^+ sputtered and annealed to ~600 °C under ultrahigh vacuum conditions (base pressure in the low 10^{-8} Pa). This resulted in clean, flat surfaces which displayed the characteristic $22\times\sqrt{3}$ herringbone reconstruction. C_{60} was loaded into a ceramic crucible and sublimed *in situ* from a Knudsen cell at temperatures of 300–360 °C. The purity of the C_{60} material (MER Corporation) was greater than 99.96%, as verified by our independent high purity liquid chromatography (HPLC) analysis. A JEOL JSTM4500S scanning tunneling microscope was used to obtain constant current images using electrochemically

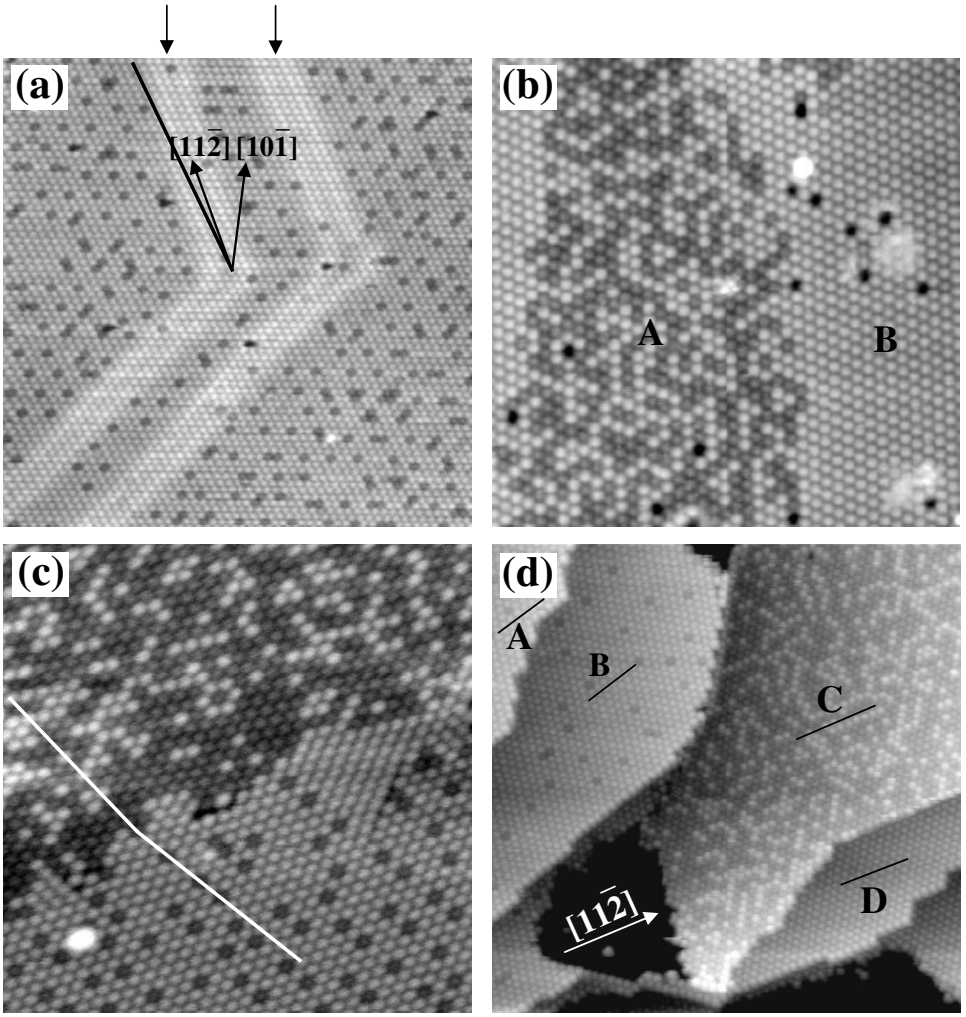

FIG. 1. A selection of room-temperature images showing the variety of C_{60} monolayer structures that can be created, where the fullerenes appear discretely bright and dim. (a) A quasiperiodic 3×3 $R34°$ superstructure formed in the absence of annealing (image size of 44.1 $\times$44.1 nm^2, V_s=+2.0 V, and I_t=0.10 nA). A black line indicates a close packed C_{60} direction, which is rotated by ~34° to the [10$\bar{1}$] direction of the Au(111) surface. Two features arising from $22\times\sqrt{3}$ reconstructed Au(111) herringbones are highlighted by downward arrows at the top of the image. (b) A disordered domain (region A) situated within a C_{60} domain of uniform height (B) (image size of 35.5 $\times$35.5 nm^2, V_s=+1.3 V, and I_t=0.20 nA). This sample had not been subjected to post-deposition annealing. (c) Two neighboring domains of disordered (top) and quasiperiodic (bottom) C_{60} arrays formed after a 410 °C anneal (image size of 25.4$\times$25.4 nm^2, V_s=+2.5 V, and I_t=0.10 nA). White lines that run parallel to the close packed directions highlight that the two domains are rotated by ~4° with respect to each other. (d) A region showing multiple Au terraces, each hosting different C_{60} domains, labeled A–D, after annealing to ~300 °C (image size of 52.6$\times$52.6 nm^2, V_s=+2.0 V, and I_t=0.10 nA). Black lines follow the C_{60} close packed directions.

etched tungsten wire tips, with the bias voltage applied to the sample. Post-deposition annealing steps were performed for one to two hours (temperatures indicated in figure captions), after which samples were cooled to room temperature prior to imaging. All images were processed using WSXM software.[39]

III. RESULTS

A. Annealing C_{60} monolayers

A variety of structures can be observed when C_{60} is deposited by sublimation onto a $22\times\sqrt{3}$ reconstructed Au(111) surface at room temperature, particularly if subjected to post-deposition annealing. Examples of such arrangements are given in Fig. 1. From this figure, it can be seen that the C_{60} molecules generally adopt a close packed arrangement. However, these STM images show that notable variations in appearance often exist between different regions, even for the same sample. Here, we will define regions of close packed C_{60} that are of the same orientation with respect to the Au(111) surface and/or are of the same global appearance as being a "domain."

In Fig. 1(a), a single domain is shown in which individual and small clusters of apparently dim fullerenes can be seen. These are situated at approximately periodic sites and are surrounded by uniformly brighter fullerenes. We will define such regions where individual or small clusters of dim C_{60} show evident periodicity, although local positional deviations

exist, as being "quasiperiodic." Two pairs of bright lines are also observed [indicated by downward arrows in Fig. 1(a)], which arise from the herringbone arrangement of Au atoms beneath the C_{60} layer.[36,37] In contrast to a clean Au(111) $22\times\sqrt{3}$ surface, these lines do not cover the entire surface. Instead, their isolated nature signifies that in other regions the C_{60} overlayer has lifted the Au(111) $22\times\sqrt{3}$ reconstruction, in agreement with studies elsewhere.[34] Figure 1(a) shows that the density of dim C_{60} is notably reduced in the vicinity of surviving herringbone patterns. In addition, the spacing between the pair of herringbone lines in Fig. 1(a) is 11 nm, significantly larger than the separation of 6.3 nm on a clean Au(111) $22\times\sqrt{3}$ surface.[40] Localized defects can also be seen in this figure, such as dark holes (missing C_{60}) and an isolated bright protrusion.

Figure 1(b) shows two regions of different appearance. Region A comprises an apparently random distribution of dim C_{60}, while the C_{60} in region B appear to be of uniform height. The molecular overlayers of both regions are approximately of the same orientation. However, since these two regions appear different by STM, we define them as separate domains. Another example of two nearby domains on the same Au terrace is given in Fig. 1(c). A quasiperiodic domain is seen toward the bottom of this image, which is of similar appearance to that in Fig. 1(a). The C_{60} in the top of Fig. 1(c) are of a similar appearance to those in domain A of Fig. 1(b). These regions have a much higher density of dim C_{60} than the quasiperiodic structures and these are arranged in a random manner; we define these regions as "disordered" domains.

Separate domains can also occur on different Au terraces, as exemplified by Fig. 1(d). In this image, several regions are seen with different arrangements of dim C_{60}. Regions A and B comprise isolated or small clusters of dim C_{60}; these are quasiperiodic domains, but have a larger average separation between the dim sites than in Figs. 1(a) and 1(c), bottom half. Region C is a disordered domain, while the fullerenes in region D are of uniform height [similar to domain B of Fig. 1(b)].

As can be seen from Fig. 1(d), the disordered and uniform C_{60} domains (regions C and D) are aligned along the $[11\bar{2}]$ directions of the Au(111) surface, while the quasiperiodic domains of regions A and B are offset by an angle of 16° from this direction. This suggests that a strong correlation exists between the appearance of a region and its orientation with respect to the Au(111) surface. We measure that the molecules within the disordered phase are of the $2\sqrt{3}\times 2\sqrt{3}$ phase, as are many of the apparently uniform height C_{60} domains. However, as can be seen upon close inspection of Fig. 1(b), very subtle offsets of less than 1° between the uniform and disordered regions often exist. In the absence of annealing, we also observe domains of apparently uniform C_{60} which are in the so-called in-phase 38×38 arrangement. Possible C_{60} positions with respect to the Au(111) lattice of the $2\sqrt{3}\times 2\sqrt{3}R30°$ and in-phase 38×38 arrangements are shown in Figs. 2(a) and 2(b). In the $2\sqrt{3}\times 2\sqrt{3}R30°$ arrangement, each C_{60} occupies an identical lattice site with respect to the underlying Au(111) surface.[34]

In addition to the orientation of the overlayer with respect to the Au(111) surface, the quasiperiodic domains display an additional superstructure which arises from the arrangement of dim fullerenes within the C_{60} arrays. We observe quasiperiodic domains with two discrete average spacings between dim fullerene clusters. Average separations of ~7 C_{60} are seen in Fig. 1(d), regions A and B, in which the molecules adopt the recently reported 7×7 $R14°$ superstructure.[35,36] A schematic of this structure is shown in Fig. 2(c). Every seventh C_{60} along the close packed directions (14° to the $[10\bar{1}]$ directions) occupies the same lattice site, consistent with the average periodicity of dim C_{60} in this type of domain.[35] In contrast, the separation of the dim fullerenes/clusters in Figs. 1(a) and 1(c) (bottom) is a significantly smaller 3.04 ± 0.07 C_{60} molecules, as determined from Fourier analyses. We believe that this is a previously unreported phase, where the C_{60} monolayer is aligned along an axis rotated 34° from the $[10\bar{1}]$ directions [Fig. 1(a)]. We denote this phase the 3×3 $R34°$ superstructure, in which every third C_{60} occupies the same lattice site. A schematic representation of the 3×3 $R34°$ superstructure is shown Fig. 2(d).

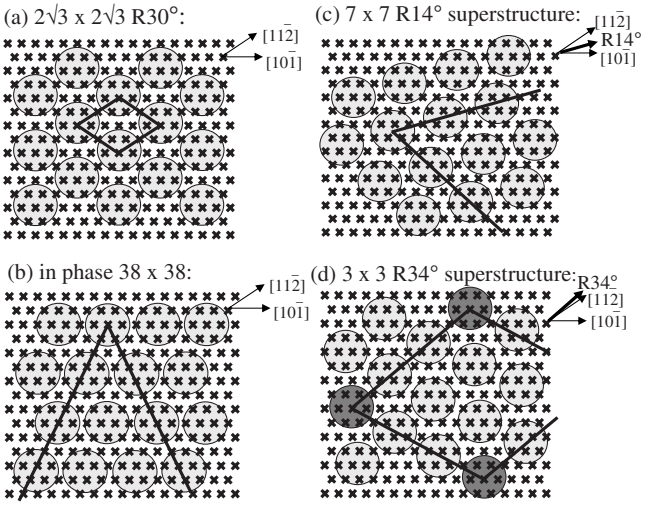

FIG. 2. Schematic representations of observed C_{60} arrangements with respect to the Au(111) lattice. Positions of C_{60} are denoted by lightly shaded circles, while Au atomic positions are represented by crosses and unit cells (whole or partial) are indicated by black lines. (a) and (b) depict the well-established $2\sqrt{3}\times 2\sqrt{3}R30°$ phase and "in-phase" 38×38 arrangements, respectively (adapted from Ref. 34). (c) Illustrates the arrangement within the quasiperiodic $7\times 7R14°$ superstructure (Refs. 35 and 36). We propose the arrangement of the 3×3 $R34°$ superstructure (d) in which every third C_{60} molecule occupies the same Au(111) lattice site, as highlighted by darker circles. The close packed C_{60} directions of the quasiperiodic phases are indicated by thick arrows.

A strong correlation exists between the domain type and annealing temperature. In the absence of a post-deposition annealing step, domains comprising uniform C_{60}, sometimes interdispersed with apparently randomly ordered isolated dim C_{60}, are seen. However, even when the sample is held at room temperature, we also observe the quasiperiodic and very occasional disordered regions [Figs. 1(a) and 1(b)]. Upon annealing, the relative abundances of the quasiperiodic and disordered phases increase [Figs. 1(c) and 1(d)], until

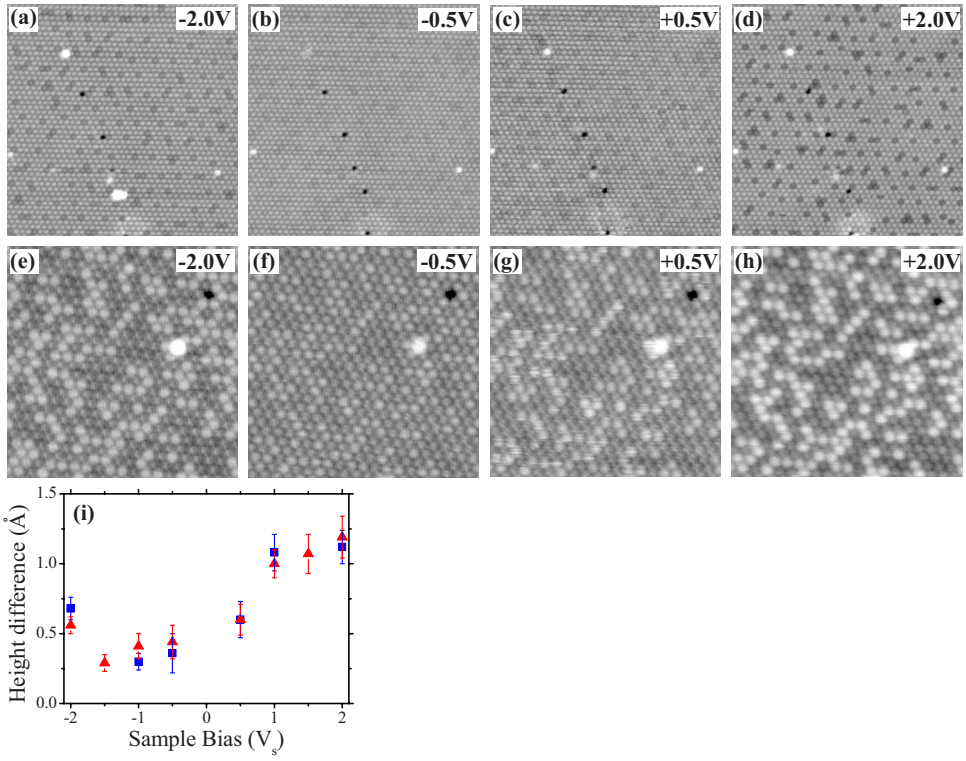

FIG. 3. (Color online) A series of bias-dependent images of two C_{60} regions: (a)–(d) a quasiperiodic phase (image size of 32.5×32.5 nm^2) and (e)–(h) a disordered phase (image size of 16.0×16.0 nm^2). The sample bias is displayed in the top right of each image, while all images were obtained with the same tunneling current (I_t=0.10 nA). The difference in apparent height of the dim and bright fullerenes varies strongly with the applied sample bias (all height scales have been constrained to cover a range of 6.0 Å). (i) A plot of the measured height difference between bright and dim C_{60} as a function of sample bias for the quasiperiodic (squares) and disordered (triangles) domains.

after annealing to temperatures of >400 °C at which the disordered structure is overwhelmingly dominant. These findings are consistent with observations of annealed C_{60} monolayers on Cu(111).[22]

B. Apparent height variation

Figure 3 shows how the applied sample bias affects the measured height difference between bright and dim C_{60}. Figures 3(a)–3(d) show STM images of the same area of a quasiperiodic array obtained at a range of applied sample biases. Figures 3(e)–3(h) use the same sample bias range but are of a disordered region. Two discrete molecular heights are measured for any given sample bias between +2.0 and −2.0 V. However, the difference between the apparent molecular heights varies strongly with the applied sample bias. Analogous trends are observed for the quasiperiodic and disordered regions, as shown in Fig. 3(i), in which the measured height differences are plotted as a function of applied sample bias. The greatest measured height difference is observed at positive sample bias where the lowest unoccupied molecular orbital (LUMO) levels dominate the tunneling process. In contrast, at small negative sample bias, the apparent height difference is significantly reduced and remains at ~0.35 Å until the highest occupied molecular orbital (HOMO) resonance is reached beyond −1.8 V.[41] We note that the trends shown in Fig. 3 are typical for any quasiperiodic or disordered domain, as has been seen reproducibly for several samples using different tips. The observed variation in apparent height with respect to bias therefore suggests that the bright and dim fullerenes have different electronic structure, with the greatest discrepancies occurring in the unoccupied levels.

C. Dynamic behavior

Consecutive STM images of quasiperiodic and disordered domains are shown in Fig. 4. By comparing successive images, it can be seen that C_{60} molecules discretely switch from bright-to-dim or vice versa. In the case of the quasiperiodic structures [Figs. 4(a_1)–4(a_3)], the fullerenes generally switch either within a cluster, or from one cluster to a neighboring one. Dim molecules are not observed between the periodic sites of the $R34°$ phase, neither are clusters of greater than four in size formed. Within disordered domains [Figs. 4(b_1)–4(b_3)], the switching generally occurs in a random manner, although pairs of bright-to-dim and dim-to-bright transitions often take place within several C_{60} units of each other, consistent with observations of C_{60} on Ag(100).[16] We have determined the rate at which C_{60} switch between bright and dim by subtracting consecutive STM images, examples of which are seen in the insets of Fig. 4. For the quasiperiodic arrays, we observe that $(3.26 \pm 0.44)\%$ of C_{60} switch from bright-to-dim after a time delay of one minute, while

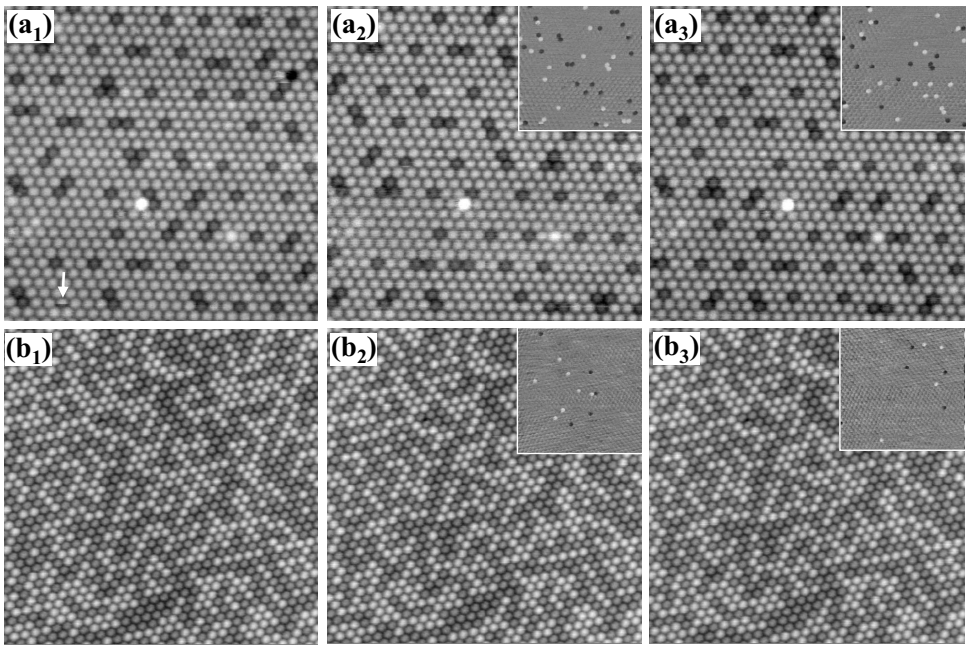

FIG. 4. A series of consecutive room temperature images of fullerene domains, in which C_{60} are seen to switch from bright-to-dim and vice versa. Images $(a_1)-(a_3)$ show a quasiperiodic domain (image size of 20.6×20.6 nm^2, 60 s separation per scan, $V_s=+2.0$ V, and $I_t=0.10$ nA), while $(b_1)-(b_3)$ are of a disordered domain (image size of 25.6×25.6 nm^2, 46 s separation per scan, $V_s=+2.0$ V, and $I_t=0.10$ nA). The insets show subtractions of consecutive images, where switching events are seen as white and dark spots corresponding to dim-to-bright and bright-to-dim transitions, respectively.

$(3.29\pm0.44)\%$ change from dim-to-bright in this timeframe. In the case of the disordered phase, we find slower switching rates of $(0.61\pm0.22)\%$ per min and $(0.61\pm0.20)\%$ per min for bright-to-dim and dim-to-bright transitions, respectively. For both arrangements, the numbers of bright and dim C_{60} are conserved with respect to time.

The time-dependent switching in the absence of a high density of holes in the C_{60} lattice demonstrates that the bright-dim contrast is not due to impurities; molecules cannot readily migrate within a close packed array unless a vacancy is present. Furthermore, the reversibility of this transition verifies that the dim fullerenes are not a result of tip-induced degradation.[42] In some cases, we observe molecules that appear half bright and half dim, an example of which is indicated by a vertical arrow in Fig. 4(a_1). Here, the molecule is seen to switch while being imaged. In order to investigate whether the switching is a tip-induced artifact, we have performed multiple time-dependent analyses using a variety of imaging conditions. We find that the switching rate is independent of the tunneling current used. Further, when pauses of 1–3 min are inserted between successive images, the number of molecules that switch also increases in a manner consistent with the aforementioned switching rates (this is harder to quantify since some C_{60} may change from bright to dim and back to bright, or vice versa, between measurements). It is therefore apparent that this switching effect is not tip induced. Interestingly, we do not observe any switching events for either phase once cooled to 77 K, suggesting that it is a kinetically driven process.

Even after the sample has been annealed to temperatures of up to ~490 °C, we have often observed small, isolated fragments of $22\times\sqrt{3}$ reconstructed Au(111) underneath the C_{60} layer. The shapes of these fragments vary and include short linear arrangements as well as more complex outlines. An example of a more complex arrangement of the herringbone lines is shown in Fig. 5. This figure comprises four consecutive images of a "templelike" feature within a disordered domain obtained at room temperature. The outline of the temple shape is characterized by pairs of bright lines similar in appearance to those in Fig. 1(a). The density of dim C_{60} in the immediate vicinity of this feature is significantly lower than in other regions, consistent with our earlier observations. At the start of this sequence, the lines toward the bottom of the temple point outwards, forming two triangular apexes [as indicated by arrows in Fig. 5(a)]. However, on a time scale of the order of a few minutes, these pairs of bright lines gradually withdraw, forming a single closed loop [Figs. 5(b)–5(d)]. Since the temple feature arises from the arrangement of the Au atoms underneath the C_{60} monolayer, this motion implies that Au atoms in the vicinity of the interface with C_{60} are not fixed and instead can rearrange themselves at room temperature.

D. Molecular orientation

The orientation of individual C_{60} molecules with respect to the Au(111) surface can be inferred from STM images in which features arising from the molecular orbitals are resolved. A selection of images of disordered and quasiperiodic domains within which the molecular orbitals can be resolved is presented in Fig. 6. At room temperature, C_{60} molecules in a bulk crystal are spinning at a rate of $\sim10^{10}$ Hz.[43,44] Therefore, our observation of orbital structure at room temperature demonstrates the existence of a sufficiently strong interaction

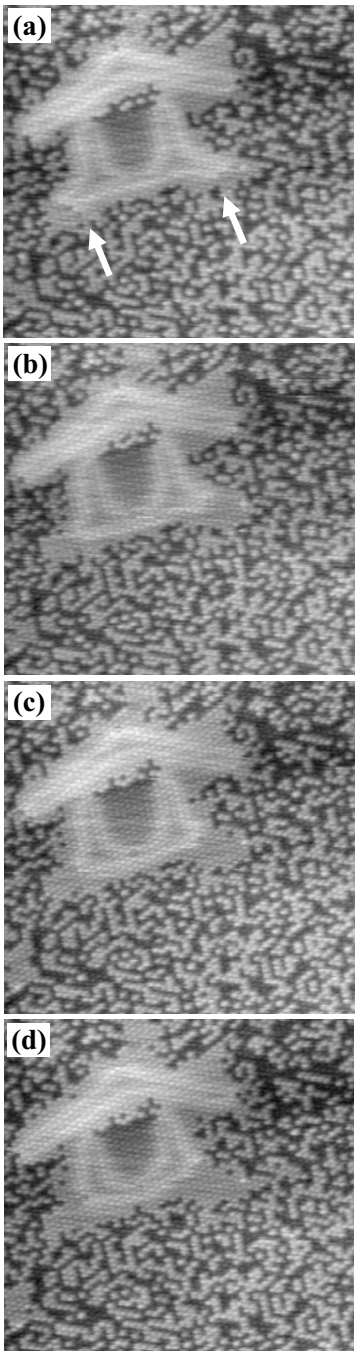

FIG. 5. Consecutive images obtained at room temperature of a region in which the Au atoms retain the $22\times\sqrt{3}$ reconstruction even after annealing to ~490 °C (image size of 42.8×43.3 nm^2, V_s=+2.0 V, and I_t=0.10 nA). (a) The first image of the sequence, within which the herringbone features at the bottom of the temple-like structure point outwards (indicated by arrows). Images (b)–(d) were taken 1 min 42 s, 5 min 6 s, and 6 min 48 s after image (a), respectively. These images show that the herringbone lines at the bottom of the temple feature close up over time to form a loop.

between the molecules and substrate to stop them from rotating. When disordered domains are imaged at negative sample bias [Fig. 6(a)], dim C_{60} adopt the appearance of a coffee bean, while the orbitals of bright C_{60} appear as three-fingered lobes. The orbital structure of the bright C_{60} in Fig.

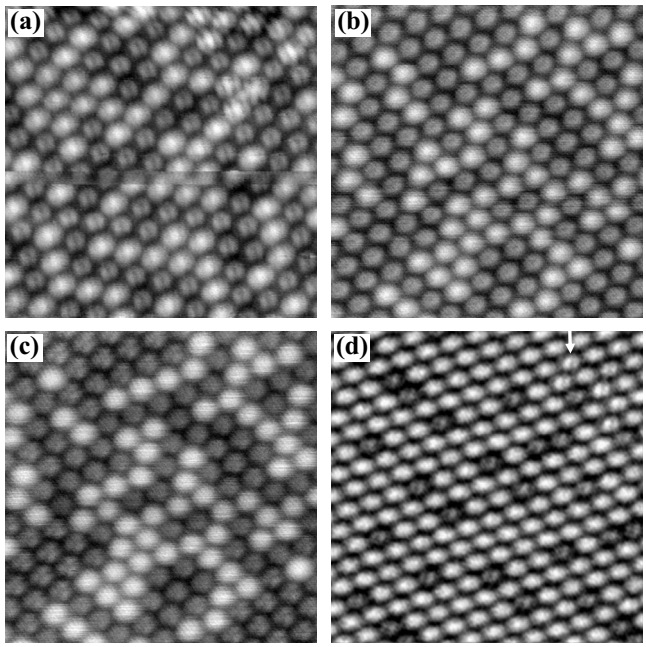

FIG. 6. Room-temperature images of C_{60} monolayers in which features arising from the molecular orbitals are resolved. (a) A disordered array showing that dim and bright fullerenes adopt different orientations (image size of 12.0×12.0 nm^2, V_s=−2.0 V, and I_t=0.30 nA). Images (b) and (c) are of the same disordered region obtained at V_s=−2.0 V and V_s=+2.0 V, respectively (image size of 10.0×10.0 nm^2 and I_t=0.30 nA). The dim C_{60} appear as three-leaf clovers at positive sample bias and like coffee beans at negative sample bias. (d) A quasiperiodic phase, within which both dim and some bright fullerenes have the same two-lobe orbital structure (an example of the latter is highlighted by a white arrow toward the top left of this image, image size of 10.9×10.9 nm^2, V_s=−2.5 V, and I_t=0.10 nA).

6(a) implies that these molecules are oriented with a 5:6 C-C bond parallel to the surface.[45] The molecular orbitals of a disordered region for negative and positive sample bias are compared in Figs. 6(b) and 6(c). The dim C_{60} of Fig. 6(b) are also of coffee bean appearance, confirming that they are of the same orientation as those in Fig. 6(a) (both images were obtained at negative bias). From Fig. 6(c), it is apparent that dim C_{60} appear as three-leaf clovers at positive bias, confirming that these molecules are arranged with a hexagonal ring parallel to the surface.[3,4]

The molecular orbital structures of C_{60} within a quasiperiodic domain can be seen from Fig. 6(d). Again, the dim molecules each have two well-defined stripes (like a coffee bean) when imaged at negative sample bias. The orbital structures of only a handful of bright fullerenes can also be resolved, for example as highlighted by an arrow in the top right of Fig. 6(d). The orbital structures of these small clusters of bright fullerenes were observed in successive images and so their appearance cannot be attributed to a momentarily improved resolution of the tip. The molecular orbitals of these bright fullerenes appear similar to those of dim C_{60}, demonstrating that bright and dim molecules can have the same orientation with respect to the substrate. This implies that the molecular orientation with respect to the substrate

alone cannot be responsible for the apparent height contrast of C_{60}, in contrast to previous reports.[32,33] Instead, it is likely that the relationship between orientation and apparent height for disordered arrays is merely a consequence of another mechanism that drives the dim-bright contrast. We note that we have not succeeded in resolving well-defined orbital structures for the remaining bright C_{60} of quasiperiodic domains. This could be due to these molecules having a weaker interaction with the substrate, thus allowing them to rotate at room temperature, or that they adsorb in a range of orientations wherein their molecular orbitals are sufficiently ill-defined.[35]

IV. DISCUSSION

We have found that domains evolve upon post-deposition annealing comprising quasiperiodic or disordered arrangements of dim C_{60}. The type of domain formed is strongly correlated with the alignment of the C_{60} array with respect to the Au substrate. These domains display a dynamic bright-dim switching behavior at room temperature, while the apparent height difference varies as a function of sample bias. We now turn our attention to identifying the mechanisms responsible for these observations. From consideration of the shape of the molecular orbitals of C_{60} within both types of domain, it is apparent that the observed height difference is not due to the molecular orientation. Further, the dim molecules cannot be due to impurities (such as C_{70}), owing to both the observed switching in the absence of holes in the close packed lattice, and the high purity of the molecular material (as verified by HPLC). Instead, it seems likely that the observed height variation is due to topographic and/or electronic differences within the C_{60} monolayer arrays. We note that C_{60} is known to induce nanopits in a variety of other metallic surfaces,[16–30] and that this could lead to topographic variations. However, the bias dependence of Fig. 3 implies that the apparently bright and dim C_{60} have different electronic properties. We will now discuss the topographic and electronic mechanisms for possible apparent height variation in more detail.

A. Au surface topography

The reconstructed clean Au(111) $22\times\sqrt{3}$ surface has 23 atoms in the surface layer for every 22 in the bulk along the $[1\bar{1}0]$ directions.[40] However, C_{60} chemisorbs onto Au(111) and has the ability to modify the substrate surface.[37] We have shown that C_{60} almost completely lifts the surface reconstruction, which is achievable at room temperature owing to the small energy difference between the reconstructed Au surface and the unreconstructed arrangement.[46] Lifting the surface reconstruction to form a bulk-terminated arrangement releases some Au atoms. However, even in the absence of step edges, the number of additional Au atoms is insufficient to lead to the high density of nanopits required for the disordered domains. Instead, a larger distortion of the uppermost Au layers is required to form significant quantities of topographically different sites. Our observations that Au atoms remaining in the $22\times\sqrt{3}$ reconstruction move beneath the C_{60} layer at room temperature, as shown in Fig. 5 and by the increased separation of the herringbone features in Fig. 1(a), confirm that the substrate atoms can reorganize underneath the C_{60} layer. It is likely that this motion is not tip induced owing to the independence of the room temperature bright-dim switching rate both upon varying the tunneling current and the insertion of pauses between imaging. We note that the density of dim C_{60} is severely reduced in the vicinity of any surviving herringbone fragments, confirming the requirement for the Au $22\times\sqrt{3}$ reconstruction to be lifted to induce a high density of dim C_{60}. Our observation of increased densities of dim C_{60} upon annealing implies that an energy barrier exists to form pits, consistent with similar observations on other surfaces.[16–25]

The correlation between domain type and rotation of the C_{60} overlayer with respect to the substrate lattice supports our claim that the bright-dim contrast is driven by the formation of pits in the Au surface. As shown in Fig. 2(d), every third C_{60} of the 3×3 $R34°$ superstructure occupies an identical position with respect to the Au(111) lattice. It therefore seems likely that C_{60}-induced nanopits in the Au surface are preferentially formed when a C_{60} occupies specific lattice sites. In a similar manner, on average every seventh C_{60} molecule of the $R14°$ quasiperiodic phase appears dim and occupies an identical lattice site.[35] Therefore, the sites at which nanopits are formed match the periodicity between the C_{60} overlayer and Au(111) lattice for both quasiperiodic phases. In contrast, disordered domains are of the $2\sqrt{3}\times2\sqrt{3}$ $R30°$ phase, where each C_{60} occupies an identical lattice site.[34] Therefore there is no advantage for the disordered phase to be periodic or that the ratio of bright to dim C_{60} should be fixed, consistent with our observations. In addition, the irreversible evolution upon increasing annealing temperature from uniform height to quasiperiodic to disordered arrays suggests the latter is the most energetically favorable arrangement. It is possible that the disordered structures will subtly shift their orientation away from the $2\sqrt{3}\times2\sqrt{3}$ phase [Fig. 1(b)] in order to maximize the commensurability with the surface and increase the number of dim C_{60}. We have not observed domains in which the C_{60} appear almost entirely dim, although this is likely to require annealing to higher temperatures, at which point the C_{60} sublime from the surface.

Further evidence for a rough Au surface beneath the fullerene layer is seen in the individual molecular orientation of the dim C_{60} molecules (as judged from the appearance of their molecular orbitals, Sec. III D). When situated within a nanopit, the molecules adopt an orientation that maximizes their interaction strength with the surrounding Au atoms, in a similar manner to that proposed for C_{60} on Au(110).[26] The pits formed for any given domain are likely to be identical, since their shape is determined by the commensurability between the C_{60} overlayer and substrate. Owing to the bias dependence of the measured apparent heights, we are unable to accurately deduce the true topographic depth of the nanopits and are therefore unable to propose a more detailed structural model for the Au-C_{60} interface for each domain type. However, the $\sim$0.35 Å height difference measured within the HOMO-LUMO gap suggests that a smaller true height variation exists than on many other metallic surfaces.

The time invariance of the ratio of bright to dim C_{60} is consistent with mass conservation of the Au atoms. The fixed total number of Au atoms means that the number of pits of any given size that can be formed at any one instance is constrained (in the absence of nearby Au terraces). This gives rise to a dynamic C_{60}-Au interface, the motion of which is frozen out when the experiments are carried out at 77 K. We note that a clean Au surface is itself dynamic; at room temperature Au atoms readily diffuse across the surface, causing Au terraces to grow at rates of 0.5–5 Å/s.[47,48] It is not unreasonable that, especially if subjected to stress from the C_{60} overlayer, the Au atoms can quickly and easily switch between different conformations, resulting in the observation of localized pairs of bright-dim transitions.[16]

B. Electronic effects

The bias dependence of the measured height differences shown in Fig. 3 cannot be explained by C_{60} occupying two discrete heights. To a first approximation one would expect a constant height difference as a function of bias if the electronic structure of the higher and the lower molecules were the same. As there is a clear bias dependence, this confirms that electronic differences exist between bright and dim C_{60}. Different orientations of C_{60} on Au(111) only lead to very subtle variations in their density of states,[3,41] while the occupation of inequivalent lattice sites leads to contrast effects only observable in differential conductance maps.[8] Instead, an alternative mechanism that leads to a significant difference in the molecular density of states must exist between the bright and dim fullerenes.

On some other metallic surfaces, such as Au(110), the dim-bright contrast is almost solely topographic and does not display any bias dependence.[28] In contrast, on other surfaces such as Cu(100) and Ag(100), the formation of nanopits leads to charge transfer to the dim C_{60}, resulting in differences in the density of states of dim and bright fullerenes.[19,23] The degree of charge transfer to C_{60} from an Au(111) surface varies, particularly at Au terraces,[8] demonstrating that the geometry of the immediate Au environment surrounding a C_{60} molecule plays an important role. We propose that once nanopits are formed, the local rearrangement of the Au(111) interface and resulting perturbation to its electronic properties are sufficient to induce charge transfer from the Au substrate to the C_{60} cage. Additional charge on C_{60} results in Jan-Teller distortions of the C_{60} cage. This lifts the degeneracy of the LUMO levels[49] and so gives rise to distinct differences between the unoccupied density of states of charged and neutral C_{60}. Even though the physical (topographic) distortion to the cage is unlikely to be measurable by STM, the electronic differences are sufficient to result in variations in the measured height difference as a function of applied sample bias. The ensuing apparent height contrast would be largest where the greatest variation in the density of states exists,[19] namely, for the unoccupied levels, as we have observed [Fig. 3(i)]. Subtle variations in the positions of the HOMO levels would also affect the apparent height difference beyond ~ -1.8 V. Due to the absence of states between the HOMO level and Fermi energy, almost no variation would be expected between the measured molecular heights in this region. Therefore, a model in which both topographic and electronic variations occur fully accounts for the bias-dependent trends of the apparent height differences between dim and bright fullerenes shown in Fig. 3.

We note that our proposal of charge transfer in this system may be considered controversial; other reports suggest that no net charge is transferred across the Au(111)-C_{60} interface. However, such studies have been largely performed on isolated C_{60} molecules deposited onto a substrate held below room temperature,[3] or involve theoretical calculations which assume an atomically flat Au surface.[38] The thermally enhanced formation of nanopits which induce charge transfer therefore resolves the discrepancies between STM-based observations in the absence of annealing, and the bulk photoelectron experiments on Au(111) where the samples are annealed to remove multilayer regions prior to measurement.[6]

V. CONCLUSIONS

We have observed a variety of structures upon annealing C_{60} on Au(111). These monolayer structures comprise discretely bright and dim fullerenes, of which a variety of arrangements have been observed. In particular, we report the formation of two classes of domain; quasiperiodic arrangements, including a 3×3 $R34°$ superstructure, and disordered arrays. We have shown that the type of structure is strongly correlated with the rotation of the overlayer with respect to the Au(111) surface. Further, we have observed a tendency toward disordered domains, which possess higher densities of dim C_{60} molecules, upon increasing annealing temperature. We propose that these dim molecules arise from the creation of nanopits in the Au surface, causing some C_{60} to be situated slightly lower than others, while this arrangement facilitates charge transfer from the Au(111) surface to C_{60} molecules. We note that our proposal of charge transfer could be verified by scanning tunneling spectroscopy or ultraviolet photoelectron spectroscopy measurements. However, all of our observations are explained by a nanopit charge-transfer model, which also accounts for the well-documented discrepancy in measured charge transfer for C_{60} monolayers on Au(111).

ACKNOWLEDGMENTS

This work is supported by the EPSRC-GB (ED/D048761/1 and GR/S15808/01). The authors thank P. Ferarri for assistance with HPLC analysis and C. Spencer (JEOL) for technical support. We are grateful to A. Q. Shaw, A. Iwasiewicz-Wabnig, V. Burlakov, and K. Porfyrakis for valuable discussions.

*Present address: Department of Physics, Harvard University, Oxford Street, Cambridge, MA 02138, USA.
†martin.castell@materials.ox.ac.uk

[1] H. W. Kroto, J. R. Heath, S. C. O'Brien, R. F. Curl, and R. E. Smalley, Nature (London) **318**, 162 (1985).
[2] T. Sakurai, X.-D. Wang, Q. K. Xue, Y. Hasegawa, T. Hashizume, and H. Shinohara, Prog. Surf. Sci. **51**, 263 (1996).
[3] X. Lu, M. Grobis, K. H. Khoo, S. G. Louie, and M. F. Crommie, Phys. Rev. B **70**, 115418 (2004).
[4] L.-L. Wang and H.-P. Cheng, Phys. Rev. B **69**, 165417 (2004).
[5] L.-L. Wang and H.-P. Cheng, Phys. Rev. B **69**, 045404 (2004).
[6] C.-T. Tzeng, W.-S. Lo, J.-Y. Yuh, R.-Y. Chu, and K.-D. Tsuei, Phys. Rev. B **61**, 2263 (2000).
[7] B. W. Hoogenboom, R. Hesper, L. H. Tjeng, and G. A. Sawatzky, Phys. Rev. B **57**, 11939 (1998).
[8] C. Rogero, J. I. Pascual, J. Gomez-Herrero, and A. M. Baro, J. Chem. Phys. **116**, 832 (2002).
[9] S. Modesti, S. Cerasari, and P. Rudolf, Phys. Rev. Lett. **71**, 2469 (1993).
[10] T. R. Ohno, Y. Chen, S. E. Harvey, G. H. Kroll, J. H. Weaver, R. E. Haufler, and R. E. Smalley, Phys. Rev. B **44**, 13747 (1991).
[11] A. J. Pérez-Jiminéz, J. J. Palacios, E. Louis, E. San Fabian, and J. A. Verges, ChemPhysChem **4**, 388 (2003).
[12] M. R. C. Hunt, S. Modesti, P. Rudolf, and R. E. Palmer, Phys. Rev. B **51**, 10039 (1995).
[13] K.-D. Tsuei, J.-Y. Yuh, C.-T. Tzeng, R.-Y. Chu, S.-C. Chung, and K.-L. Tsang, Phys. Rev. B **56**, 15412 (1997).
[14] T. Hashizume, K. Motai, X. D. Wang, H. Shinohara, Y. Saito, Y. Maruyama, K. Ohno, Y. Kawazoe, Y. Nishina, H. W. Pickering, Y. Kuk, and T. Sakurai, Phys. Rev. Lett. **71**, 2959 (1993).
[15] A. J. Maxwell, P. A. Bruhwiler, D. Arvanitis, J. Hasselstrom, M. K.-J. Johansson, and N. Martensson, Phys. Rev. B **57**, 7312 (1998).
[16] C.-L. Hsu and W. W. Pai, Phys. Rev. B **68**, 245414 (2003).
[17] E. Giudice, E. Magnano, S. Rusponi, C. Boragno, and U. Valbusa, Surf. Sci. **405**, L561 (1998).
[18] W. W. Pai and C.-L. Hsu, Phys. Rev. B **68**, 121403(R) (2003).
[19] X. Zhang, W. He, A. Zhao, H. Li, L. Chen, W. W. Pai, J. Hou, M. M. T. Loy, J. Yang, and X. Xiao, Phys. Rev. B **75**, 235444 (2007).
[20] M. Grobis, X. Lu, and M. F. Crommie, Phys. Rev. B **66**, 161408(R) (2002).
[21] C. Cepek, R. Fasel, M. Sancrotti, T. Greber, and J. Osterwalder, Phys. Rev. B **63**, 125406 (2001).
[22] W. W. Pai, C.-L. Hsu, M. C. Lin, K. C. Lin, and T. B. Tang, Phys. Rev. B **69**, 125405 (2004).
[23] M. Abel, A. Dmitriev, R. Fasel, N. Lin, J. V. Barth, and K. Kern, Phys. Rev. B **67**, 245407 (2003).
[24] P. W. Murray, M. O. Pedersen, E. Laegsgaard, I. Stensgaard, and F. Besenbacher, Phys. Rev. B **55**, 9360 (1997).
[25] R. Felici, M. Pedio, F. Borgatti, S. Iannotta, M. Capozi, G. Ciullo, and A. Stierle, Nature Mater. **4**, 688 (2005).
[26] M. Hinterstein, X. Torrelles, R. Felici, J. Rius, M. Huang, S. Fabris, H. Fuess, and M. Pedio, Phys. Rev. B **77**, 153412 (2008).
[27] M. Pedio, R. Felici, X. Torrelles, P. Rudolf, M. Capozi, J. Rius, and S. Ferrer, Phys. Rev. Lett. **85**, 1040 (2000).
[28] J. K. Gimzewski, S. Modesti, and R. R. Schlittler, Phys. Rev. Lett. **72**, 1036 (1994).
[29] J. Weckesser, C. Cepek, R. Fasel, J. V. Barth, F. Baumberger, T. Greber, and K. Kern, J. Chem. Phys. **115**, 9001 (2001).
[30] J. Weckesser, J. V. Barth, and K. Kern, Phys. Rev. B **64**, 161403(R) (2001).
[31] G. Costantini, S. Rusponi, E. Giudice, C. Boragno, and U. Valbusa, Carbon **37**, 727 (1999).
[32] E. I. Altman and R. J. Colton, Surf. Sci. **295**, 13 (1993).
[33] E. I. Altman and R. J. Colton, Phys. Rev. B **48**, 18244 (1993).
[34] E. I. Altman and R. J. Colton, Surf. Sci. **279**, 49 (1992).
[35] G. Schull and R. Berndt, Phys. Rev. Lett. **99**, 226105 (2007).
[36] X. Zhang, F. Yin, R. E. Palmer, and Q. Guo, Surf. Sci. **602**, 885 (2008).
[37] J. K. Gimzewski, S. Modesti, C. Gerber, and R. R. Schlitter, Chem. Phys. Lett. **213**, 401 (1993).
[38] J. D. Sau, J. B. Neaton, H. J. Choi, S. G. Louie, and M. L. Cohen, Phys. Rev. Lett. **101**, 026804 (2008).
[39] I. Horcas, R. Fernandez, J. M. Gomez-Rodriquez, J. Colchero, J. Gomez-Herrero, and A. M. Baro, Rev. Sci. Instrum. **78**, 013705 (2007).
[40] J. V. Barth, H. Brune, G. Ertl, and R. J. Behm, Phys. Rev. B **42**, 9307 (1990).
[41] G. Schull, N. Neel, M. Becker, J. Kroger, and R. Berndt, New J. Phys. **10**, 065012 (2008).
[42] G. Schulze, K. J. Franke, and J. I. Pascual, New J. Phys. **10**, 065005 (2008).
[43] R. D. Johnson, C. S. Yannoni, H. C. Dorn, J. R. Salem, and D. S. Bethune, Science **255**, 1235 (1992).
[44] D. A. Neumann, J. R. D. Copley, R. L. Cappelletti, W. A. Kamitakahara, R. M. Lindstrom, K. M. Creegan, D. M. Cox, W. J. Romanow, N. Coustel, J. P. McCauley, N. C. Maliszewskyj, J. E. Fischer, and A. B. Smith, Phys. Rev. Lett. **67**, 3808 (1991).
[45] J. J. Pascual, J. Gomez-Herrero, C. Rogero, A. M. Baro, D. Sanchez-Portal, E. Artacho, P. Ordejon, and J. M. Soler, Chem. Phys. Lett. **321**, 78 (2000).
[46] Y. Wang, N. S. Hush, and J. R. Reimers, Phys. Rev. B **75**, 233416 (2007).
[47] R. C. Jaklevic and L. Elie, Phys. Rev. Lett. **60**, 120 (1988).
[48] R. Emch, J. Nogami, M. M. Dovek, C. A. Lang, and C. F. Quate, J. Appl. Phys. **65**, 79 (1989).
[49] D. Arcon and R. Blinc, Struct. Bonding (Berlin) **109**, 231 (2004).